Journal of the Formosan Medical Association (2014) 113, 680–687

Available online at www.sciencedirect.com

SciVerse ScienceDirect

journal homepage: www.jfma-online.com

ORIGINAL ARTICLE

An efficient method for decellularization of the rat liver

Ming Xin Pan [a,b,d], Peng Yun Hu [c,d], Yuan Cheng [a,b,d], Li Quan Cai [a,b], Xiao Hui Rao [a,b], Yan Wang [a,b,*], Yi Gao [a,b,*]

[a] *Department of Hepatobiliary Surgery, Southern Medical University, Guangzhou, Guangdong Province, China*
[b] *Institute of Regenerative Medicine, Zhujiang Hospital, Southern Medical University, Guangzhou, Guangdong Province, China*
[c] *Department of Tumor Surgery, Xinxiang Central Hospital, Xinxiang, Henan Province, China*

Received 28 April 2012; received in revised form 3 May 2013; accepted 9 May 2013

KEYWORDS
biocompatibility;
decellularization;
liver organ

Background/Purpose: Using gradient ionic detergent, we optimized the preparation procedure for the decellularized liver biologic scaffold, and analyzed its immunogenicity and biocompatibility.
Methods: EDTA, hypotonic alkaline solution, Triton X-100, and gradient sodium dodecyl sulfate (1%, 0.5%, and 0.1%, respectively) were prepared for continuous perfusion through the hepatic vascular system. The decellularization of the liver tissue was performed with the optimized reagent buffer and washing protocol. In addition, the preservation of the original extracellular matrix was observed. To analyze its biocompatibility, the scaffold was embedded in a heterologous animal and the inflammation features, including the surrounding cell infiltration and changes of the scaffold architecture, were detected. The cell-attachment ability was also validated by the perfusion culture of HepG2 cells with the scaffold.
Results: By using gradient ionic detergent, we completed the decellularization process in approximately 5 h, which was shorter than >10 hours in previous experiments ($p < 0.001$). The extracellular matrix was kept relatively intact, with no obvious inflammatory cellular infiltration or structural damage in the grafted tissue. The engraftment efficiencies of HepG2 were $86 \pm 5\%$ ($n = 8$). The levels of albumin and urea synthesis were significantly superior to the ones in traditional two-dimensional culture.
Conclusion: The current new method can be used efficiently for the decellularization of the liver biologic scaffold with satisfying biocomparability for application both *in vivo* and *in vitro*.

Conflicts of interest: The authors have no conflicts of interest relevant to this article.

* Corresponding authors. Department of Hepatobiliary Surgery, Zhujiang Hospital, Southern Medical University, Number 253, Industry Road, Haizhu District, Guangzhou, Guangdong Province, China.
E-mail addresses: nn1012@gmail.com (Y. Wang), gaoyi6146@163.com (Y. Gao).
[d] M.X. Pan, P.Y. Hu, and Y. Cheng contributed equally to this work.

0929-6646/$ - see front matter
http://dx.doi.org/10.1016/j.jfma.2013.05.003

Introduction

Preparation of intact three-dimensional scaffolds by decellularization is a significant breakthrough in biological scaffold preparation,[1] that has been proven possible in a variety of tissues and organs.[2–7] This approach has also shown great progress in liver tissue engineering.[8–13] There has been no standard protocol for the preparation of decellularized bioscaffolds, and a current topic of debate is which detergent has any obvious advantage in their preparation.[14,15]

The goal of this study was to completely elute cellular components using the method that is most gentle, which was achieved by emphasizing and further defining sodium dodecyl sulfate (SDS) concentrations. From the use of a single concentration in earlier studies to the establishment of a gradient, we managed to maintain the efficacy of decellularization using ionic detergents at the minimum dose and the lowest concentration. At the same time, we analyzed the decellularization efficiency by assessing perfusion through different routes according to the anatomical structure of the hepatic canalicular system.

One reason for developing a decellularization technique is to achieve the transmission of tissues and organs across species; for example, the adaptation of decellularized tissues and organs from large animals for use in humans. The theoretical basis of this application is that the extracellular matrix components are of low immunogenicity between species. Currently, the research into whole-liver bioscaffolds focuses on the preparation of whole-liver scaffolds, recellularization of the scaffold tissues, and monitoring of transplantation among homogeneous species.[8] There has been no report on rejection responses against decellularized liver tissues in heterologous animals. In the current study, by preparing decellularized liver tissues and embedding them in the muscle tissues of heterologous animals, inflammatory infiltration and structural preservation were monitored. The potential biocompatibility of the decellularized liver tissue was verified.

Materials and methods

Experimental animals and reagents

Forty specific pathogen-free (SPF) male or female Sprague-Dawley (SD) rats, weighing 200—300 g, and 20 New Zealand white rabbits, weighing 1.9—2.5 kg, were purchased from the Experimental Animal Center of the Southern Medical University [Certification: SCXK (Guangdong) 20060015]. Animal use during the study followed "The Guidance for the Treatment of Laboratory Animals" published by the Ministry of Science and Technology in 2006.

HepG2 cells, a human liver carcinoma cell line,[16] were a gift from the Guangzhou Institute of the Chinese Academy of Science. Tris-HCl buffer was prepared and used as a solvent to prepare 1% Triton X-100 (Sigma-Aldrich, St. Louis, MO, USA) and SDS (1%, 0.5%, and 0.1%). D-Hanks medium was prepared and used to prepare EDTA (Sigma-Aldrich).

The isolation of liver from SD rats

SD rats ($n = 10$) were anesthetized by intraperitoneal injection of chloral hydrate, followed by topical skin disinfection. A transverse incision was made in the abdomen, which exposed the portal vein, the bile duct, and the inferior vena cava. A total of 2 mL heparin sodium was injected for anticoagulation. The branches of the portal vein were ligated. The portal vein was then cut with a side hole for intubation and double-fixed with number 1 silk sutures. The hepatic superior and inferior vena cava were isolated and both were cut with a side hole for intubation. The inferior vena cava was then transected and the whole liver was isolated.

Liver decellularization by different routes

First, the portal vein was perfused with D-Hanks medium containing 0.02% EDTA and then with 1% Triton X-100 for approximately 1 hour. After rinsing with 500 mL phosphate buffered saline (PBS), the liver was perfused sequentially with 500 mL 1%, 0.5%, and 0.1% SDS, followed by a wash with PBS. The perfusion rate for each step was 10 mL/min. Additional fresh liver samples ($n = 10$) were perfused through the inferior vena cava in the same order as mentioned previously. The prepared biological scaffolds were preserved in PBS at 4°C.

Analyzing ECM components of the whole-liver bioscaffolds

The samples were randomly collected from scaffolds, and the tissue sections were analyzed with hematoxylin and eosin (H&E) and Masson trichrome staining. Scanning electron microscopy (SEM) was used to observe the microstructure of the ECM.

The samples were collected from decellularized bioscaffolds and fresh liver and embedded, sectioned, dehydrated with gradient ethanol, and then incubated with 1:100 diluted primary rabbit antirat fibronectin or rabbit antirat laminin antibodies (Boster Biological Technology Ltd., Wuhan, China). This step was followed by the addition of secondary biotinylated goat antirabbit antibodies (Boster Biological Technology Ltd.) and visualization with diaminobenzidine. The ECM components were analyzed by Western blot analysis with the indicated primary antibodies, including anticollagen I, anticollagen III, antifibronectin, and antilaminin (Boster Biological Technology Ltd.), and horseradish peroxidase-conjugated secondary antibodies. The dilution ratio of the antibodies used was based on the manufacturer's recommendations.

Analyzing the vascular system of the whole-liver bioscaffolds

The 8—10% filler (containing red dye) was prepared in perchloroethylene and acetone and was slowly infused into the portal vein or the inferior vena cava. The preservation of the vascular structure of the whole-liver bioscaffolds was observed, and the local leakage of casting agents was monitored.

Biocompatibility analysis of the decellularized liver bioscaffolds in heterologous animals

The samples were collected randomly from the whole scaffolds, and the tissue blocks were incubated in 0.1% peracetic acid at 37°C for 3 hours on a shaker at 300 rpm. Then, the tissue blocks were washed with PBS for 15 minutes with shaking at 300 rpm. A 2-cm incision was made on the back of New Zealand white rabbits ($n = 20$), and a tissue block approximately 1 cm in diameter and 3 mm in thickness was embedded in the back muscles (the size of samples was based on BS/EN/ISO standards). The surgical procedure was performed in sterile conditions, and the dressings were changed every day after surgery. Additionally, 80,000 units of penicillin were applied for 3 consecutive days after suture, once in the morning and once in the evening. The control group ($n = 20$) was from the same batch, had the same body weight, and was notched on the back as a sham surgery. The condition of eating and drinking was monitored daily, and blood samples were collected daily for assessment of C-reactive protein (CRP) and immunoglobulin E (IgE; Table 1).

Biocompatibility evaluation with HepG2 culture

To simulate the environment *in vivo*, we constructed a circulation perfusion culture device loaded with the decellularized liver scaffold, including a peristaltic pump, bubble remover, oxygenator. The portal venous structure was connected with the circulation and was the medium inlet, with a patent hepatic vein. HepG2 cells were seeded using the method by Uygun et al,[8] and a total of 100×10^6 cells were injected into the scaffold via the portal vein in four steps, with 15-minute intervals between each step. The perfusion culture was carried out at a rate of 5 mL/min. The temperature was 37°C, and continuous ventilation was maintained with 95% oxygen and 5% carbon dioxide. The medium was changed every 2 days. The engraftment rate was calculated from the total number of implanted cells minus the number of cells floating in the medium.

Statistical analyses

Statistical analysis was carried out using SPSS version 13.0 (SPSS Inc. Chicago, IL, USA). Results were expressed as mean ± standard deviation (SD). Statistical differences of cell functions between perfusion culture and two-dimensional culture were evaluated by Student *t* test. A p value < 0.05 was considered statistically significant.

Table 1 Comparison of C-reactive protein and immunoglobulin E after transplantation of scaffold.

	Surgery group ($n = 20$)	Control group (mg/L) ($n = 20$)	p
CRP (mg/L)	0.12 ± 0.03	0.14 ± 0.05	0.1672
IgE (IU/L)	4.1 ± 0.4	3.6 ± 0.6	0.9260

Data are presented as mean ± SD.
CRP = C-reactive protein; IgE = immunoglobulin E.

Results

The decellularization process of liver organ

By using a decellularization perfusion device, it could be seen that the liver color gradually changed, from the blood flushing out of the liver (Fig. 1A), to the liver turning yellowish-brown, and ending in transparency (Fig. 1B). The entire process took approximately 5 hours. Through the capsule of the prepared whole-liver scaffold, the Glisson system, portal vein, and the biliary tract could be seen.

Liver decellularization with different routes

The bioscaffolds prepared from perfusion through the portal vein or the inferior vena cava showed the same decellularized efficiency (Fig. 1D–F). It cost less perfusion gradient during perfusion (mean, 4100 mL vs. 7000 mL, $p < 0.001$), and the time for perfusion to transparency was significantly shorter than our previous procedure and that of Uygun et al[8] (mean, 5 hours vs. 12 hours and 5 hours vs. 52 hours, $p < 0.001$).[17]

The ECM components of whole-liver bioscaffolds were well preserved

Comparison of H&E-stained normal livers (Fig. 2A) and decellularized whole-liver bioscaffolds (Fig. 2B) showed no residual cells in the decellularized samples. From the comparative analysis of Masson trichrome staining (Fig. 2C and D), most of the collagen fiber components of the ECM were retained and the collagen fibers maintained tubular structures. Under SEM, residual cells were also not found (Fig. 2J), and the major (Fig. 2L) and minor vascular branches (Fig. 2K) were observed in the bioscaffolds. Immunohistochemical analysis indicated the presence of fibronectin and laminin in the bioscaffolds (Fig. 2F and H) when compared to these two ECM components from fresh liver (Fig. 2E and G). The results from Western blot analyses showed the preservation of collagen I, collagen III, fibronectin, and laminin in the decellularized bioscaffolds (Fig. 2I). According to the experimental data, there were no significant differences between the experimental and control groups.

The vascular system in the whole-liver bioscaffolds was well preserved

As shown in Fig. 3, by slowly infusing with red casting agent through the portal vein, the main branch of the vascular system was seen first. With the advancement of the casting agent, the microvascular structures were gradually revealed. There was no leakage of casting agents through the vascular walls, suggesting that the decellularization procedure did not cause damage to the vascular structure.

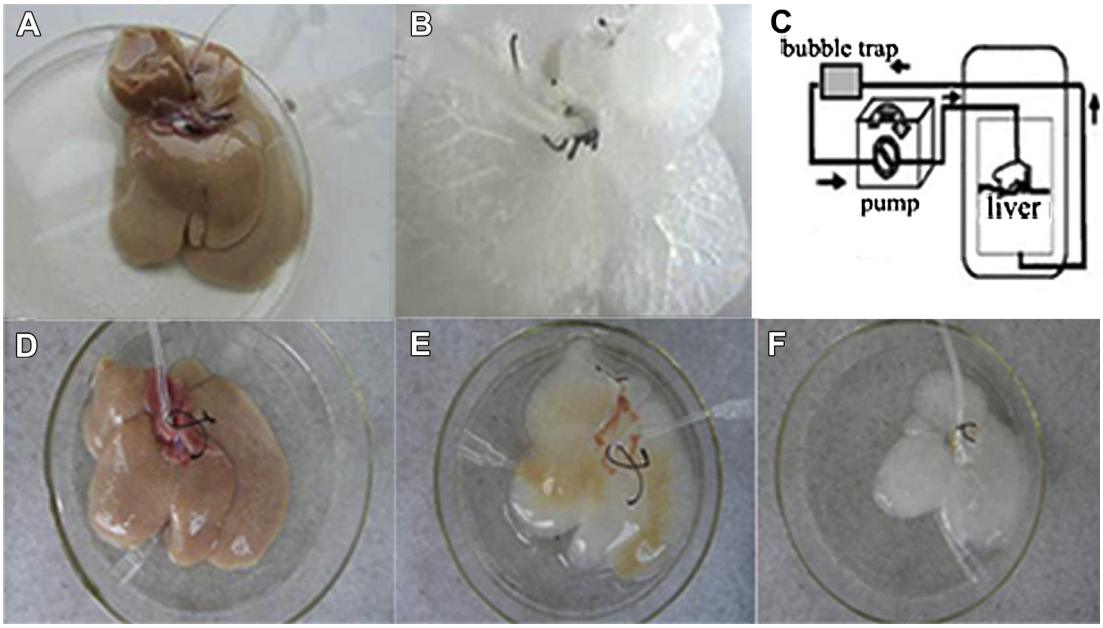

Figure 1 (A) Fresh rat liver. (B) Decellularized scaffold. (C) Perfusion device diagram in decellularization. (D—F) Macroscopy of the liver at decellularization, 5 minutes (D), 2 hours (E) and 5 hours (F).

The decellularized liver bioscaffolds showed good compatibility in heterologous animals

After surgery, the animals showed normal behavior in regard to eating and drinking. The blood samples were collected for 7 days to determine the level of CRP and IgE. Compared to the control group, there was no significant difference in CRP (mean, 0.12 ± 0.03 mg/L vs. 0.14 ± 0.05 mg/L, $t = 1.414$, $p = 0.1672$) and IgE (mean, 4.1 ± 0.4 k IU/L vs. 3.6 ± 0.6 k IU/L, $t = 1.0$, $p = 0.926$). At 2 weeks ($n = 10$) and 4 weeks ($n = 10$) after embedding, the implanted tissue samples were harvested. The decellularized rat liver tissues appeared white and softer in texture. H&E staining of tissue sections is shown in Fig. 4A and C. Additionally, Wright staining of the tissue samples was performed at 2 weeks and 4 weeks of embedment. As shown in Fig. 4B and D, infiltrated inflammatory cells were still present at the conjunction of the implanted liver tissues and the back muscle tissues at 2 weeks of embedment. Nevertheless, the border between the experimental samples and the muscle tissues was well defined at 4 weeks of embedment, with no obvious infiltration. Meanwhile, Masson trichrome staining (Fig. 4E and F) showed the extensive presence of collagen fibers, revealing no apparent structural changes.

Function of HepaG2 cultured within the decellularized scaffold

A total of eight perfusion culture experiments were carried out to implant HepG2 cells. The average engraftment efficiency was $86 \pm 5\%$. We measured albumin and urea levels

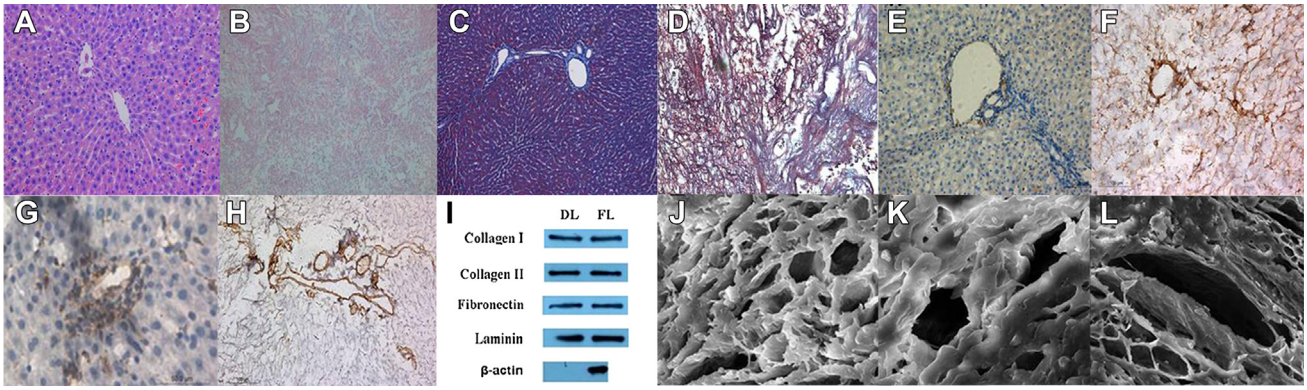

Figure 2 (A—H) Histologic comparison of normal liver (A,C,E,G) and decellularized liver matrix (B,D,F,H): hematoxylin and eosin staining (A—B); Masson trichrome staining (C—D); immunohistochemistry staining of fibronectin (E—F) and laminin (G—H). Western blot showed the expression of collagen I, collagen II, fibronectin, and laminin, which was compatible with normal liver (I). (J—L) Extracellular matrix showed invisible cells in decellularized matrix (J), matrix retains an intact tiny lobular structure (K) and main vasculature (L). Magnification: A—F 100×; G—H 200×; J and K 3000×; L 1200×.

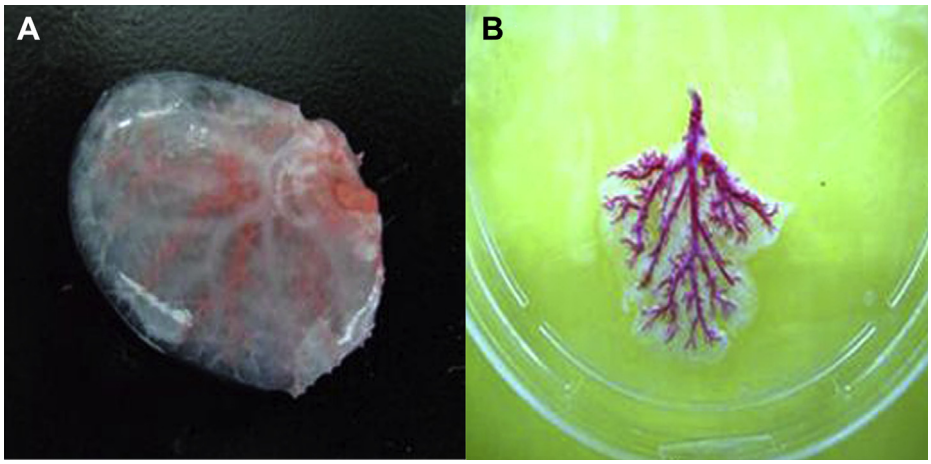

Figure 3 Cast model of one liver lobe demonstrates the integrity of (A) the hepatic vein and (B) the portal vein.

to evaluate the function of cells in the scaffold and the results showed that the 7-day cumulative albumin synthesis and urea secretion in HepG2 cells after perfusion culture were significantly higher than that after two-dimensional culture (albumin synthesis, $27.5 \pm 1.7\ \mu g/10^6$ cells vs. $19.0 \pm 1.4\ \mu g/10^6$ cells, $p < 0.001$; urea secretion, $14.5 \pm 2.5\ \mu mol/10^6$ cells vs. $12.7 \pm 1.1\ \mu mol/10^6$ cells, $p < 0.05$) (Fig. 5A and B). On Day 5 of culture, HepG2 cells were distributed throughout the scaffold (Fig. 5C). The results showed that HepG2 perfusion culture is superior to conventional two-dimensional culture.

Discussion

Scaffold materials not only provide ample space for cellular colonization, expansion, and proliferation, but they also provide morphology control in two- and three-dimensional

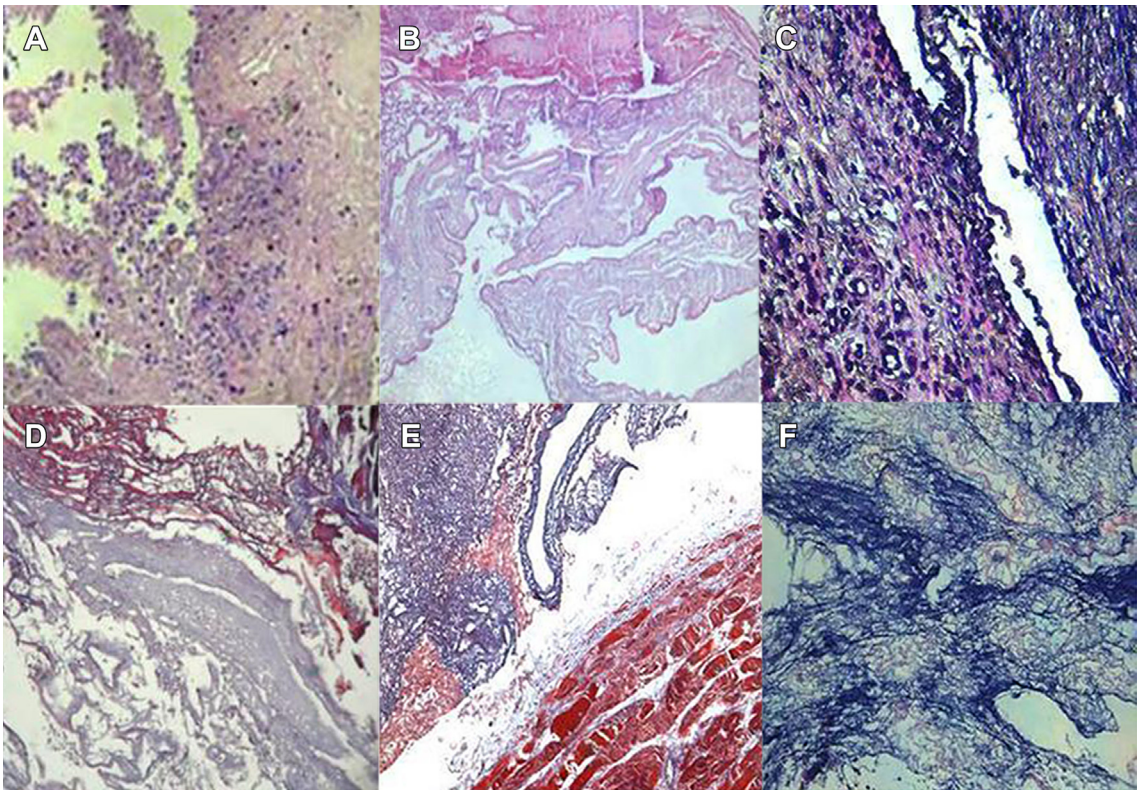

Figure 4 (A and C) Histologic change after the embedding performed at 2 weeks and (B and D) at 4 weeks. (A and B) Hematoxylin and eosin staining. (C and D) Wright staining showed there were still some inflammatory cells at the boundary of the implanted matrix, but with no obvious infiltration at 4 weeks. (E and F) Masson trichrome staining showed the collagen fibers were largely preserved in the boundary (E) and center (F) of the implanted matrix. Magnification: A, B, and E 100×; C, D, and F 200×.

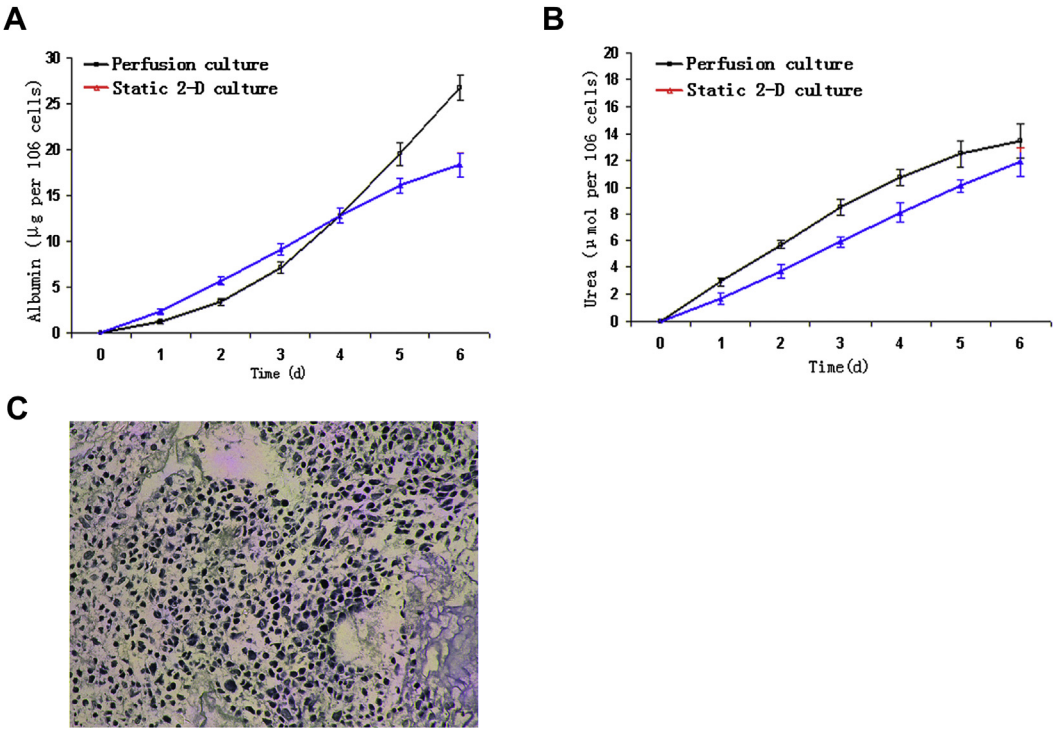

Figure 5 Function of the recellularized liver graft *in vitro*. (A) Albumin synthesis and (B) urea secretion of HepG2 cells, in comparison with static two-dimensional culture ($p < 0.05$ for albumin and urea, by Student t test). $n = 8$.

cell culture.[18] In liver tissues, the ECM components not only regulate cell adhesion, migration, differentiation, proliferation, etc, but they also transmit signal transduction between different cells.[19] In the process of decellularization, both the decellularization efficiency and the preservation of the ECM need to be taken into account. This requires the application of a detergent demonstrating highly efficient elution and tissue-destructive activity.

Considering the combinational characteristics of the liver (such as complicated structure, copious cells, and abundant cellular enzymes) we chose continuous perfusion with detergent containing EDTA, hypotonic alkaline solution, Triton X-100, and SDS for decellularization. EDTA dissociated the junctions between the cells as well as the cells and the ECM. TritonX-100 acted mildly, preventing a sudden enzyme burst from the massive cell destruction, which might have caused damage to the ECM. However, its decellularization activity was not thorough and required an adequate amount of SDS for enhancement. The currently used approach for decellularization usually relies on a higher dosage of ionic detergents to guarantee decellularization. The advantage of our elution procedure was to ensure decellularization efficiency with the use of a minimum amount of ionic detergents critical to the integrity of the ECM components and structures, yet finishing the preparation of whole-liver bioscaffolds in the shortest amount of time. In addition, the decreased dosage of SDS could gradually diminish the residual of SDS in the scaffold; meanwhile, it reduced the volume of PBS for rinsing out of the ionic detergent. Therefore, we chose this modified method rather than previous methods.

In regard to the different routes for perfusion, we found that due to the smaller hepatic artery and bile duct of rats, a longer perfusion time tended to cause tube detachment and the increased pressure could lead to bile duct breakage. The portal vein had the advantages of suitable vascular diameter, easy exposure, and not being easily twisted after intubation. According to the analysis by Baptista et al[10] on perfusion via the portal vein system or inferior vena cava system, the sites of concentration and action of the eluting agent were different inside the hepatic lobule. Therefore, different perfusion routes might lead to different eluting efficiencies. In our study, both perfusion routes (the portal vein and the inferior vena cava) were investigated. Both showed similar elution effects and took approximately 5 hours, the shortest time among current studies in the same field.[8,9] In addition, although these two perfusion routes showed no differences, we could rule out the possibility that combining forward and reverse routes in large animals might increase perfusion efficiency.

The ECM components are usually produced and secreted by resident cells in the tissues and organs, and they are maintained in dynamic homeostasis with the surrounding environment.[20] Because the ECM is produced by the original resident cells of each tissue and organ, it is theoretically an ideal cell substrate.[21–24] ECM is a complex composed of multiple structural and functional molecules arranged in tissue-specific and three-dimensional structural order.[25–27] The ECM components, including collagens, are highly conserved between species, and therefore do not usually cause obvious immune responses.[28,29]

The decellularized liver bioscaffolds are completely free of cellular components and theoretically will not induce apparent immune rejection. However, it cannot be completely ruled out that the different components of the ECM between heterologous animals might induce the

production of heterologous antibodies. During the preparation of bioscaffolds, the completeness of decellularization, the differences in ECM components, and the complicated intrinsic environment of the recipients can affect potential immunogenicity and inflammatory responses. To verify these factors, preliminary investigation of the rejection response against the liver tissue scaffolds in the heterologous animals was undertaken.

Following implantation of the decellularized liver bioscaffolds derived from SD rats into the back muscles of New Zealand white rabbits, cellular infiltration and structural destruction surrounding the embedded tissue blocks were monitored at different time points. According to the hematological index, it was concluded that the decellularized liver tissue did not induce apparent immune rejection in the heterologous animals.

Since Uygun et al[8] first reported successful culture of hepatocytes in decellularized liver scaffold in 2010, more studies have reported that the decellularized liver scaffold is superior to the previous iteration. Our study provided a safe and operational basis for the application of decellularized rat liver bioscaffolds. Perfusion culture with HepG2 was rarely reported. The results showed that cells grew well in the decellularized liver scaffold and revealed the good biocompatibility between heterologous animals and provided the possibility for tissue reengineering. However, due to the complexity of the liver structure, more investigations are needed to address the major issues in this area, such as the standardized protocols for the decellularization of large animals, and the bioreactors design and culture protocols for recellularization.

Acknowledgments

This study was supported by Science and Technology Projects of Guangdong Province (2011B031800127) and National High Technology Research and Development Program of China ("863" Program 2012AA020505). The authors are grateful to Rang Ke Wu for editing of the manuscript and translation assistance.

References

1. Badylak SF. The extracellular matrix as a scaffold for tissue reconstruction. *Semin Cell Dev Biol* 2002;**13**:377—83.
2. Yoo JJ, Meng J, Oberpenning F, Atala A. Bladder augmentation using allogenic bladder submucosa seeded with cells. *Urology* 1998;**51**:221—5.
3. Dahl SL, Koh J, Prabhakar V, Niklason LE. Decellularized native and engineered arterial scaffolds for transplantation. *Cell Transplant* 2003;**12**:659—66.
4. Nieponice A, Gilbert TW, Badylak SF. Reinforcement of esophageal anastomoses with an extracellular matrix scaffold in a canine model. *Ann Thorac Surg* 2006;**82**:2050—8.
5. Schechner JS, Crane SK, Wang F, Szeglin AM, Tellides G, Lorber MI, et al. Engraftment of a vascularized human skin equivalent. *FASEB J* 2003;**17**:2250—6.
6. Macchiarini P, Jungebluth P, Go T, Asnaghi MA, Rees LE, Cogan TA, et al. Clinical transplantation of a tissue-engineered airway. *Lancet* 2008;**372**:2023—30.
7. Ott HC, Matthiesen TS, Goh SK, Black LD, Kren SM, Netoff TI, et al. Perfusion-decellularized matrix: using nature's platform to engineer a bioartificial heart. *Nat Med* 2008;**14**:213—21.
8. Uygun BE, Soto-Gutierrez A, Yagi H, Izamis ML, Guzzardi MA, Shulman C, et al. Organ reengineering through development of a transplantable recellularized liver graft using decellularized liver matrix. *Nat Med* 2010;**16**:814—20.
9. Shupe T, Williams M, Brown A, Willenberg B, Petersen BE. Method for the decellularization of intact rat liver. *Organogenesis* 2010;**6**:134—6.
10. Baptista PM, Siddiqui MM, Lozier G, Rodriguez SR, Atala A, Soker S. The use of whole organ decellularization for the generation of a vascularized liver organoid. *Hepatology* 2011;**53**:604—17.
11. Barakat O, Abbasi S, Rodriguez G, Rios J, Wood RP, Ozaki C, et al. Use of decellularized porcine liver for engineering humanized liver organ. *J Surg Res* 2012;**173**:e11—25.
12. Zhou P, Lessa N, Estrada DC, Severson EB, Lingala S, Zern MA, et al. Decellularized liver matrix as a carrier for the transplantation of human fetal and primary hepatocytes in mice. *Liver Transpl* 2011;**17**:418—27.
13. Bao J, Shi Y, Sun H, Yin X, Yang R, Li L, et al. Construction of a portal implantable functional tissue-engineered liver using perfusion-decellularized matrix and hepatocytes in rats. *Cell Transplant* 2011;**20**:753—66.
14. Cartmell JS, Dunn MG. Effect of chemical treatments on tendon cellularity and mechanical properties. *J Biomed Mater Res* 2000;**49**:134—40.
15. Woods T, Gratzer PF. Effectiveness of three extraction techniques in the development of a decellularized bone-anterior cruciate ligament-bone graft. *Biomaterials* 2005;**26**:7339—49.
16. Aden DP, Fogel A, Plotkin S, Damjanov I, Knowles BB. Controlled synthesis of HBsAg in a differentiated human liver carcinoma-derived cell line. *Nature* 1979;**282**:615—6.
17. Kang YZ, Wang Y, Gao Y. Decellularization technology application in the whole liver reconstruct biological scaffold. *Natl Med J China* 2009;**89**:1135—8.
18. Kulig KM, Vacanti JP. Hepatic tissue engineering. *Transpl Immunol* 2004;**12**:303—10.
19. Svegliati-Baroni G, De Minicis S, Marzioni M. Hepatic fibrogenesis in response to chronic liver injury: novel insights on the role of cell-to-cell interaction and transition. *Liver Int* 2008;**28**:1052—64.
20. Bissell MJ, Aggeler J. Dynamic reciprocity: how do extracellular matrix and hormones direct gene expression? *Prog Clin Biol Res* 1987;**249**:251—62.
21. Mirsadraee S, Wilcox HE, Watterson KG, Kearney JN, Hunt J, Fisher J, et al. Biocompatibility of acellular human pericardium. *J Surg Res* 2007;**143**:407—14.
22. Ozeki M, Narita Y, Kagami H, Ohmiya N, Itoh A, Hirooka Y, et al. Evaluation of decellularized esophagus as a scaffold for cultured esophageal epithelial cells. *J Biomed Mater Res A* 2006;**79**:771—8.
23. Sellaro TL, Ravindra AK, Stolz DB, Badylak SF. Maintenance of hepatic sinusoidal endothelial cell phenotype in vitro using organ-specific extracellular matrix scaffolds. *Tissue Eng* 2007;**13**:2301—10.
24. Lin P, Chan WC, Badylak SF, Bhatia SN. Assessing porcine liver-derived biomatrix for hepatic tissue engineering. *Tissue Eng* 2004;**10**:1046—53.
25. Laurie GW, Horikoshi S, Killen PD, Segui-Real B, Yamada Y. In situ hybridization reveals temporal and spatial changes in cellular expression of mRNA for a laminin receptor, laminin, and basement membrane (type IV) collagen in the developing kidney. *J Cell Biol* 1989;**109**:1351—62.
26. Baldwin HS. Early embryonic vascular development. *Cardiovasc Res* 1996;**31**:e34—45.

27. Rabinovitch M. Cell-extracellular matrix interactions in the ductus arteriosus and perinatal pulmonary circulation. *Semin Perinatol* 1996;**20**:531—41.
28. Van der Rest M, Garrone R. Collagen family of proteins. *FASEB J* 1991;**5**:2814—23.
29. Allman AJ, McPherson TB, Merrill LC, Badylak SF, Metzger DW. The Th2-restricted immune response to xenogeneic small intestinal submucosa does not influence systemic protective immunity to viral and bacterial pathogens. *Tissue Eng* 2002;**8**: 53—62.